Proc. of the 9th International Symposium on Geotechnical Safety and Risk (ISGSR)
Edited by Zhongqiang Liu, Jian Dai and Kate Robinson
Published by Research Publishing, Singapore. ©2025 The Author(s), CC-BY 4.0 licence.
doi: 10.3850/GRF-25280825_isgsr-009-P367-cd

SEISMIC SITE RESPONSE OF REGIONS IN NORTHERN BIHAR

R V S Jenny Laura

Department of Civil Engineering, Indian Institute of Technology Guwahati, India.
E-mail: jennylaura.ks@gmail.com

Abhileen Chatterjee

Centre for Disaster Management and Research, Indian Institute of Technology Guwahati, India.
E-mail:chatterjee.abhi15@gmail.com

DasariNithin

Department of Civil Engineering, Indian Institute of Technology Guwahati, India.
E-mail: nithindasari001@gmail.com

Abhishek Kumar

Department of Civil Engineering, Indian Institute of Technology Guwahati, India.
E-mail: abhiak@iitg.ac.in

Due to the proximity of northern Bihar to the great Himalayan collision arc, the region has been exposed to hundreds of moderate to great earthquakes (EQs) since prehistoric times, leading to devastating effects. Understanding of such regions in the light of seismic site response is critical. To do so, initially, Multichannel Analysis of Surface Wave (MASW) and Standard Penetrationtesting (SPT) are coupled in understanding the subsurface properties of selected sites. The obtained shear wave velocity (V_s) profiles and borelog data from the site are extrapolated to a depth of 100 m. Further, 12 synthetic bedrock motions are generated using EXSIM due to the lack of regional ground motion (GM) records for the locality. These extrapolated dynamic soil properties and synthetic ground motions (SGMs) are incorporated into the equivalent linear site response analysis (ELSRA) algorithm. Based on the analysis, the influence of Peak horizontal acceleration (PHA) and impedance contrast (IC) on amplification factors (AFs) are discussed. Furthermore, the impact of variation of depth on surface manifestation is highlighted. Such understanding of site response to EQs, influences the choice of ground improvement techniques and subsequent seismic hazard mitigation activities.

Keywords: Synthetic ground motion; Equivalent linear site response; site investigation; Amplification factor

1. Introduction

The Himalayan Rangeexperiences strain accumulation due to theinter-plate collision of the tectonic plates. Despite its tectonic activity, the region has not experienced major EQsrecently, resulting in multiple seismic gaps: the Kashmir Gap, the Assam Gap, and the Central Seismic Gap. Specifically, the Central Seismic Gap, spanning between the 1905 KangraEQ and the 1934 Bihar-Nepal EQ, has been under the spotlight due to lack of major seismic activity. Bilham (2019) highlighted that the region holds the potential to produce an EQ of 8.7 (Mw) if it slips as a single event.Bihar, lying adjacent to the Central Seismic Gap, has experienced notable EQs, including the 2015 Gorkha EQ and 1934 Bihar-Nepal EQ Bilham (2019).Liquefaction is one of the predominant surface manifestations pertaining to the EQs(Sukhija et al. 2002). Ground response analysis (GRA) is critical in comprehending such local site effects (LSEs) (Bajaj and Anbazhagan 2019b). Coupling noninvasive exploration techniques like MASW and SPT has been proven to estimate the near surface properties (Bajaj and Anbazhagan 2019a) for GRA. At times when arriving at shallow subsurface profiles, due to experimental limitation, extrapolation of profile is executed. Wang and Wang (2015) outlined one of the V_s profile extrapolation methods that utilizes time averaged shear wave velocity $\bar{V}_S$. Another limitation, specific to the CentralSeismic Gap is the lack of availability of regional GMs. Pertaining to the same, Boore (2003) developed methods to generate SGMs to support seismic studies. On incorporating the above explained methodologies, an attempt to estimate the LSE of selected regions at proximity to Central Seismic Gap is carried out.

2. Soil Properties Approximation

Based on the past liquefaction instances reported bySukhija et al. (2002), four locationscollectively from Madhubani and Darbhanga are selected for the study. To understand the dynamic properties, MASWexploration

is performed in two locations. Geophones of 4.5 Hz against sampling frequencies of 3750 and 7500 Hz are used for data acquisition. Four stackings are performed at every site to reduce the error on multiple channel record. On subjecting the site data to preprocessing, dispersion curves are obtained, which on inversion yields the V_s profiles of the sites. Additionally, physical properties are estimated from the three boreholes (BHs) drilled (two 30 m and one 100 m) where SPT is executed. Obtained soil columns from MASW are denoted as L_1 and L_2, and the two 30 m BH profiles are denoted as BH_1 and BH_2. Similarly, the 100 m BH is denoted BH_{100}. The experimental soil profiles reached the depths of 47.5 m for L_1 and 30m for L_2. Deep soil profiles (100 m) are generated through extrapolation. For BH_1 and BH_2, the process involves conversion of SPT N to $V_s$at each stratification by choosing the suitable SPT-N-V_s correlation, followed by estimation of V_s at target depths using $\bar{V}_S$ of preceding depths. The linear correlation stipulated by Bajaj and Anbazhagan (2019a) for Bihar region is incorporated for the conversion of uncorrected SPT-N to V_s. The correlation is applicable till SPT N of 70 and used stratification information till the depth of 100m during formulation. For L_1 and L_2, the existing site profile for shallow depth is directly used. Deploying the V_s, the $\bar{V}_S$at depths Z_1 and Z_2 preceding the depth of interest (Z) are estimated. Using the equation provided by Wang and Wang (2015), the $\bar{V}_S$ at Z is calculated. From $\bar{V}_S$(Z), individual V_s is reverse engineered to arrive at the extrapolated V_s profiles up to 100 m. These V_s profiles are analyzed against appropriate GMs to estimate the LSE.

3. Synthetic Ground Motions Generation

The study employs the EXSIM algorithm that had been successfully used in previous studies to simulate GM records for Himalayan earthquakes (NHand Kumar, 2020; Rajaram et al. 2025). A total of 12 SGMs pertaining to two regional seismic events – the 1934 Bihar-Nepal EQ, and the 2015 Gorkha EQ are generated at three different locations namely Madhubani, Darbhanga and Sitamarhi. The simulated ground motions have been generated both for the bedrock and site class D conditions (Bajaj andAnbazhagan, 2019a). Only crustal AFs, according to Boore (2003), are considered for bedrock motions. The site class D amplified motions include an additional site-amplification parameter as discussed by Bajaj and Anbazhagan, (2019b). The hypocentral distances are calculated using the Haversine formula (referring to the works by Torbol and Shinozuka, 2014).

Due to the lack of recorded motions from the above-mentioned pair of earthquakes, the GMs from 1991 Uttarkashi EQ recorded at Almora station in India are used to validate the simulation approach. Rajaram et al., (2025) claims that a comparison with recorded motions ensures the accuracy of the method in representing the characteristics of a real GM. Figure 1(a) below shows the spectral acceleration matching of both the recorded motion and SGM pertaining to 1991 Uttarkashi EQ, at the bedrock level. The residual curves in figure 1 (b) demonstrate that the difference in spectral acceleration values between the recorded and the simulated motions at the surface are in the order of 10^{-2} g. Such low values of residual PSA show the closeness of the recorded and simulated ground motions for site class D conditions pertaining to the 1991 Uttarkashi event. The residual trend in figure 1b further corroborates with that of NHand Kumar, (2020) with regards to Himalayan earthquakes. Thus, the SGM(s) used in the paper are substantially validated with recorded ground motions for both bedrock and site class D conditions.

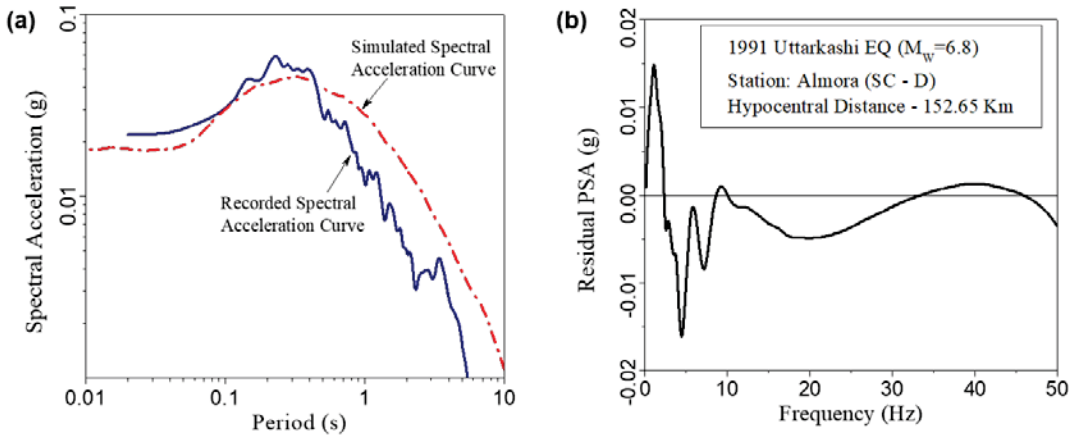

Fig 1: (a) Graphical representation of the two spectral acceleration curves from the recorded GMs (blue solid line) and the SGM (red dashed line) respectively for the 1991 Uttarkashi EQ at bedrock level. (b) residual analysis to quantify the matching of the SGM and the recorded ground motions at site class D conditions from 1991 Uttarkashi EQ

4. Site Response Analysis

The influence of the generated SGMs on the extrapolated soil columns ofBH_1, BH_2, L_1 and L_2 are evaluated using ELSRA (Kumar and Mondal, 2017). Till the depth of 30 m of soil column,the engineering properties (plasticity index, OCR etc.)are approximated based on BH_1 and BH_2. Beyond 30 m, the above-said properties are deployed from BH_{100}. Zhang et al. (2005) curves are utilized to define the modifications in dynamic soil properties – damping ([2]) and shear modulus (G) pertaining to variation of shear strain ([3]). Applicability of the curves is limited to [3] of $1x10^{-4}$ to 1%, which also accommodates the expected [3] of the current problem. Additionally, the curve incorporates the overburden pressurein the form of mean effective confining pressure. Further, the generated SGMs are incorporated such that the V_s at the base of the soil column is sensitive to the GMs applied. Owing to the same, BH_2 is subjected to six bedrock motions while the other columns are analyzed against six SC-D motions.The response of the soil column subjected to SGMs is recorded in the form of peak ground acceleration (PGA) at the surface. Further, to understand the contribution of individual stratification in the soil column, the process is repeated to obtain the peak acceleration at the top of each stratum. Finally, on utilizing the PGA and the PHA of the SGM, the AFs experienced by the strata is estimated.

5. Results and Discussions

Four locations are selected based on past liquefaction instances in northern Bihar. The sites are subjected to MASW exploration and BH drilling alongside SPT to acquire subsurface profiles. The maximum depth of subsurface profile obtained is 47.5 m for L_1. To comprehend the influence of deeper profiles in LSE, the experimental soil profiles are extrapolated till 100 m depth. The extrapolation method deploys time averaged V_s to approximate the stratification information at the depth of interest. Further, pertaining to the lack of regional GM records, SGMs are generated, six each for SC-D and bedrock conditions.Further, ELSRA is executed for the soil columns against the 6 SGMs. Fig. 2 (a-d) depicts the plots of variation in AF with respect to depth for the soil columns.

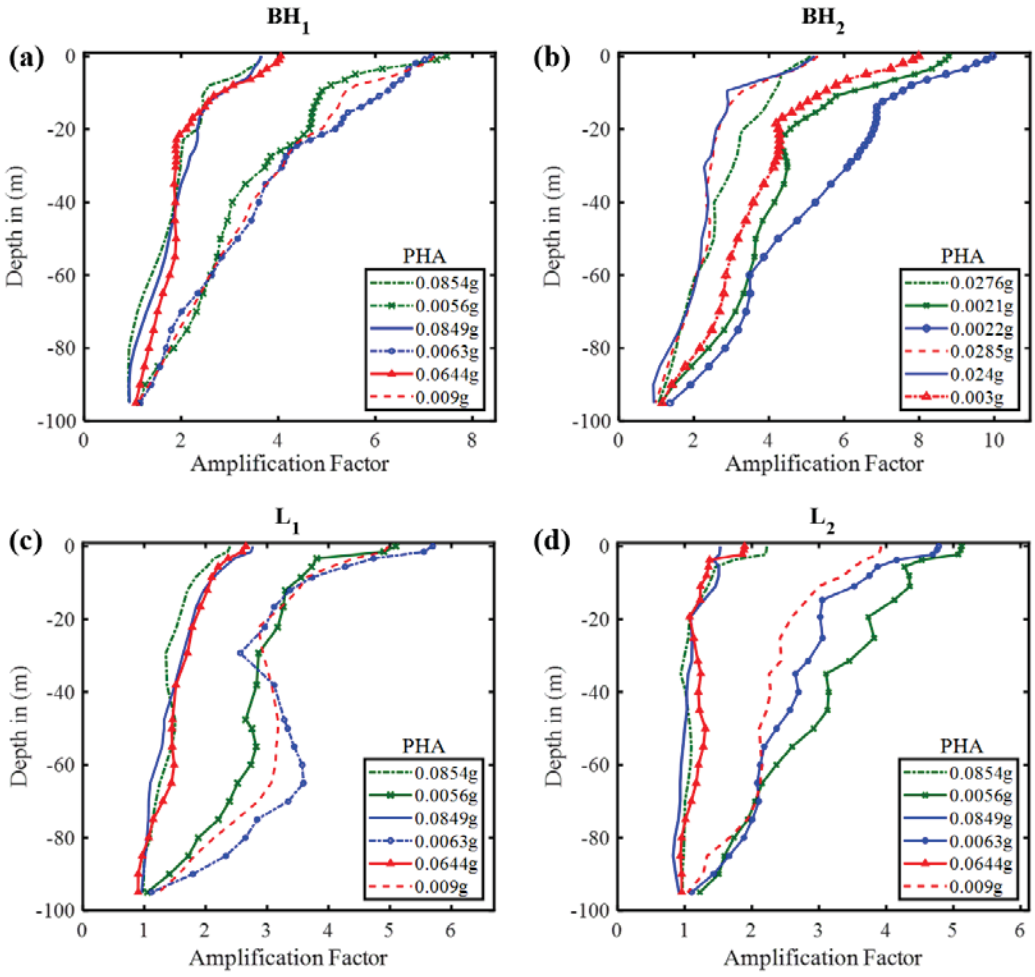

Fig 2: Graphical representation of variation of AF with respect to depth corresponding to different SGMs for (a) BH_1, (b) BH_2, (c) L_1 and (d)L_2

The legends of subplots in fig.2 enlist the PHAs of the respective SGMs incorporated.According to Fig. 2(a) at depth 0 m, the lowest PHA of 0.0056g exhibits highest AF of 7.47. Whereas the highest PHA of 0.085 g exhibits lowest AF of 3.65. Exposure to high PHA subjects the soil column to high ^{3}. Owing to the same, a decrease in AF is observed as the strata experiences high ^{2} at high ^{3}.Although the highest AFs of 7.47, 9.95,5.696 and 5.109 are observed corresponding to BH_1, BH_2, L_1 and L_2, the practical significance of such AFs are low. Such a stipulation stands valid as the PGA corresponding to the said AFs range from 0.02g to 0.04g. On the contrary, low AFs of 3.64, 5.10, 2.4 and 1.525 imparts a PGA of 0.31g, 0.1g, 0.2g and 0.13g corresponding to BH_1, BH_2, L_1 and L_2.On comparing Fig. 2 (a) and 2(d) it is also observed that,same PHA of 0.085 g results in PGAs of 0.3 g and 0.2 g corresponding to BH_1 and L_1, outlining the effects of subsurface properties.

The influence of the subsoil in modifying the AF is explored by observing the variation in IC. For BH_1,ICs of 2.32 and 20.626 are witnessed at the base and the toprespectively. Similarly, for BH_2 an IC of 2.18 and 17.17 is witnessed near the bedrock and the top of the column. Similar observations can be drawn for $L_1$and L_2. Such variation highlights the increase in IC from the bedrock to the topsoil. Such an increase in IC results in the increase in AF from the base of the soil column and the surface (fig.2). The observations are found comparable with the stipulations of Baise et al. (2016) for Boston and Eskandarinejad et al. (2023) for arbitrary bedrock overlain by soft soil criteria.

6. Conclusion

ELSRA is carried out for four soil columns (BH_1, BH_2, L_1 and L_2) in northern Bihar adjacent to Central Seismic Gap, against SGMs generated. For the purpose, initially, MASW explorations and SPT are executed in the said sites. V_s extrapolation is performed to arrive at the subsoil profile till 100 m. Additionally, six SGMs each, aligning with bedrock and SC-D conditions are generated. On subjecting the soil columns to the SGMs, LSE is quantified for the soil columns. The response of BH_1 reveals the potential of sites to impart a highest PGA of 0.31g corresponding to PHA of 0.085 g. Further for the same PHA of 0.085g, BH_1 and L_1 produced different PGAs of 0.31g and 0.2g respectively. This observation outlines the surface manifestation is not solely influenced by the PHA of the GM, but a collective phenomenon influenced by the subsurface properties. Contribution of the subsoil in modifying the SGMs is explored through the variation in IC with respect to depth. It is observed that the IC ranges from 2.32 to 20.626 at the base and top of BH_1. This reveals that the increase in IC results in the increase in AF from the base to the topsoil. The observations are found comparable with existing literature. Further, the obtained PGAs can be utilized to evaluate the liquefaction potential of the sites to provide the mitigation measures.

References

Baise, L. G., Kaklamanos, J., Berry, B. M., & Thompson, E. M. (2016). Soil amplification with a strong impedance contrast: Boston, Massachusetts. Engineering Geology, 202, 1-13.

Bajaj, K., &Anbazhagan, P. (2019, April). Seismic site classification and correlation between VS and SPT-N for deep soil sites in Indo-Gangetic Basin. Journal of Applied Geophysics, 163, 55–72.

Bajaj, K., &Anbazhagan, P. (2019, December). Comprehensive amplification estimation of the Indo Gangetic Basin deep soil sites in the seismically active area. Soil Dynamics and Earthquake Engineering, 127, 105855.

Bilham, R. (2019). Himalayan earthquakes: A review of historical seismicity and early 21st century slip potential. In Geological Society Special Publication (Vol. 483, Issue 1, pp. 423–482). Geological Society of London.

Boore, D. M. (2003). Simulation of Ground Motion Using the Stochastic Method. Pure Appl. Geophys., 160.

Eskandarinejad, A., Shiau, J., &Keawsawasvong, S. (2023). Effect of Depth-Dependent Shear Wave Velocity Profiles on Site Amplification. Transportation Infrastructure Geotechnology, 10(6), 1255-1283.

Kumar, A., & Mondal, J. K. (2017). Newly Developed MATLAB Based Code for Equivalent Linear Site Response Analysis. Geotechnical and Geological Engineering, 35(5), 2303–2325.

Nh, H., & Kumar, A. (2020). Ground motion prediction equation for north India, applicable for different site classes. *Soil Dynamics and Earthquake Engineering*, *139*, 106425. https://doi.org/10.1016/j.soildyn.2020.106425

Rajaram, C., Vemuri, J. P., Rambha, S., &Bande, G. R. (2025). A comparative study of ground motion parameters at bedrock and surface level in Kathmandu Basin. *Natural Hazards*. https://doi.org/10.1007/s11069-025-07181-8

Sukhija, B. S., Rao, M. N., Reddy, D. V, Nagabhushanam, P., Kumar, D., Lakshmi, B. V, & Sharma, P. (2002). Palaeoliquefaction evidence of prehistoric large/great earthquakes in North Bihar, India. In Science (Vol. 83, Issue 8).

Torbol, M., &Shinozuka, M. (2014). The directionality effect in the seismic risk assessment of highway networks. Structure and Infrastructure Engineering, 10(2), 175–188.

Wang, H.Y. and Wang, S.Y., (2015). A new method for estimating VS (30) from a shallow shear-wave velocity profile (depth< 30 m). Bulletin of the Seismological Society of America, 105(3), pp.1359-1370.

Zhang, J., Andrus, R. D., &Juang, C. H. (2005). Normalized Shear Modulus and Material Damping Ratio Relationships. Journal of Geotechnical and Geoenvironmental Engineering, 131(4), 405–534.